

Performance Analysis of Small Scale Variable Pitch Vertical Axis Wind Turbine

Dr. Ramesh K. Kavade

Professor in Mechanical Engineering
Department
Dr. D. Y. Patil Institute of Technology, Pimpri
Pune, Maharashtra
India

Dr. Pravin M. Ghanegaonkar

Principal & Professor in Mechanical
Engineering Department
Keystone School of Engineering
Pune, Maharashtra
India

In this paper, the changeable pitching method is used to improve the Vertical Axis Wind Turbine (VAWT) power output for electric energy generations to partially meet the energy needs for domestic use in a place where continuous wind flow is available. The preset or unchangeable pitch turbines cannot start on their own because of negative tangential force acting on the blades of the turbine. Therefore, the variable pitching method is introduced to solve the starting problem of wind turbines and increase the turbine's efficiency in the form of a power coefficient. The cam and follower variable pitch method is employed for the present analysis. In this research paper, the analytical analysis is done with the momentum stream tube model named as DMST model. The turbine model is tested, and the test results show that the power coefficient (C_p) increases with tip speed ratio, and a maximum power coefficient of about 0.35 is obtained at $\lambda = 2.5$ at 10 m/s wind speed.

Keywords: Small Scale Wind Turbine, Momentum Stream Tube Representation, Power Coefficient, Wind Speed, Pitch angle, Tip Speed Ratio

1. INTRODUCTION

The attention toward wind energy increased due to the diminution of fossil fuels and increased electrical energy demand due to rapid urbanization and the industrial revolution. The abundant availability of wind energy free of cost is an excellent option for generating electric power through wind turbine technology.

According to the orientation of the axis, the wind turbine is classified into two main groups, namely, Horizontal Axis Wind Turbine (HAWT) and Vertical Axis Wind Turbine (VAWT). Horizontal Axis Wind Turbine power plants are usually installed in coastal or hilly areas, far away from electricity use. The transmission lines are required to bring the generated electricity from the power plants to isolated places. Biadgo et al. [1] analyzed horizontal axis wind turbines by using a basic visual program. He presented an aerodynamic analysis of HAWT using the momentum stream tube model with elementary blade assumption. Performance of existing horizontal axis wind turbine is carried out with this interface program. Rasuo et al. [2] and [3] explained the wind farm and the most favorable locations of wind turbines in the wind farm for maximum usefulness. They gained the maximum power output from the turbine. Inherent algorithms are used in this paper to determine the best location of the wind turbine in the wind farm.

Vertical Axis Wind Turbines are simple in construction, low cost, and can take the wind from any direction, as their axis is perpendicular to wind flow. The complicated yaw mechanism is not required due to

the vertical facing of blades to wind flow. The maintenance of the turbine is easy due to its location near the ground. The Vertical Axis Wind Turbines can be mounted on the roof of a house, near to ground in the park, or in the garden to generate electricity independently [4-5]. Many researchers have developed and proposed the different variety of VAWTs over the past few decades. G. J. Darrieus, a French Engineer, first developed Darrieus turbine and Darrieus patented his design in 1926. Toni et al. [6] optimized Darrieus type vertical axis wind turbine using the genetic algorithm (GA). The airfoil shape is characterized using the Class-Shape Transformation (CST) method. Biadgo et al. [7] carried out numerical and analytical performance analysis of straight blade fixed pitch turbine with NACA 0012 airfoil. The turbine model using ANSYS FLUENT simulation is done for two-dimensional unsteady flow around the turbine by solving Reynolds averaged Navier-Stokes equations. Tareq et al. [8] explained energy generation by wind turbines located on the highway. The wind flow generated from the vehicle movements is used to rotate the wind turbine to generate electrical energy. The performance of these highway turbines is given in the research paper. Svorcan et al. [9] used an analytical method to the determination of the performance of the turbine. The finite element technique is referred to for structural analyses of composite blades of the turbine. Rasuo et al. [10] presented the harmonization of the new wind turbine rotor blades development process. The wind turbine with the blade of composite materials is tested for its performance. The wind turbine is designed, fabricated, and tested to understand its behavior under the various wind speeds. The various tests like; fatigue, vibratory and static tests for blades of composite materials are carried out for its performance analysis.

Many researchers for the different pitch angles varying with the sinusoidal curve analyzed the perfor-

Received: November 2021, Accepted: February 2022

Correspondence to: Dr. R. K. Kavade, Faculty of Mechanical Engineering, Dr. D. Y. Patil Institute of Technology, Pimpri, Pune, India

E-mail: kawade.ramesh@gmail.com

doi:10.5937/fme2201322K

© Faculty of Mechanical Engineering, Belgrade. All rights reserved

FME Transactions (2022) 50, 322-330 322

mance of the variable pitch turbine. The different variable pitch methods like; centrifugal force created by the balancing of mass and springs in passive pitching methods, four-bar linkages, and multi body simulation approach for active pitching methods are implemented by many researchers [11-14]. Many researchers are concentrated on the precise prediction of wind turbine performance with the help of various computational and numerical models. The different computational models with their strengths and weaknesses are available to analyze turbines [15-20]. Based on the literature review and limitations of the pitching of turbine blades with the sinusoidal curve, it is understood that there is scope for the improvement of the performance of the turbine with a modified design of the pitching scheduled to pitch the turbine blades made to order pitch angles. In a present research paper, the modified pitching angles of turbine blades are designed and suggested to the improvement of the performance of the turbine. This method of pitching blades will generate maximum torque at the blades to improve the turbine's performance in terms of coefficient of power.

2. ANALYTICAL MODEL: MOMENTUM STREAM TUBE MODEL

The analytical momentum model used for performance analysis is shown in Figure 1. The turbine blade passes through multiple streams in two parts, namely the front stream and the rear stream. The model is known as the double multiple stream tube model as it has multiple stream tube passes, separated into two streams front stream and rear stream. [21-22].

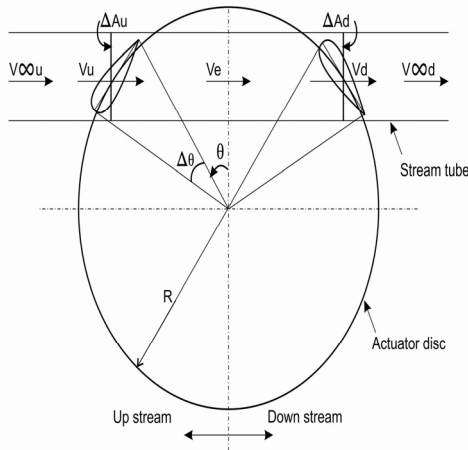


Figure 1. Momentum Analytical Method (Double Multiple Stream Tube)

The open incoming wind velocity in the front streamside ($V_{\infty u}$) is represented in Figure 1 and is reduced by the interference factor (a_u) in the line of the stream. The reduced velocity is calculated by induced rate (V_u). It is estimated for the front streamside as,

$$V_u = V_{\infty u} a_u \quad (1)$$

Similarly, equilibrium induced velocity (V_{θ}) within the front stream and rear streamside is obtained as,

$$V_{\theta} = V_{\infty u} (2a_u - 1) \quad (2)$$

Also, induced wind velocity on rear streamside (V_d) is calculated as,

$$V_d = V_{\theta} a_d \quad (3)$$

Also,

$$V_d = V_{\infty u} (2a_u - 1) a_d \quad (4)$$

This equation a_d is a factor of interference for the rear stream side of the turbine.

The following equation presents the wind velocity left from the side of the rear stream ($V_{\infty d}$) as,

$$V_{\infty d} = V_{\theta} (2a_d - 1) \quad (5)$$

Also,

$$V_{\infty d} = V_{\infty u} (2a_u - 1)(2a_d - 1) \quad (6)$$

Drag acting on turbine blade along crossways areas ΔA_u and ΔA_d is calculated by following equations as

$$F_u = \rho V_u (V_{\infty u} - V_{\theta}) \Delta A_u \quad (7)$$

Also,

$$F_u = \rho 2a_u V_{\infty u}^2 (1 - a_u) h R \sin \theta \Delta \theta \quad (8)$$

and,

$$F_d = \rho V_d (V_{\theta} - V_{\infty d}) \Delta A_d \quad (9)$$

Also,

$$F_d = \rho V_d (V_{\theta} - V_{\infty d}) h R \sin \theta \Delta \theta \quad (10)$$

The mass density (ρ) of wind is not variable across the turbine and is considered constant within the rotor flow. Therefore, wind flow across the rotor is incompressible. The performance analysis of the turbine is evaluated by considering geometrical terms such as h = height of turbine blade, R = turbine radius, B = number of turbine blades, and A swept area of the turbine. The wind comes in contact with turbine blades when it flows across it and hence, generates drag and lift on the blades of the turbine to make it rotate. The α is calculated by using the following equation,

$$\alpha = \sin^{-1} \left(\frac{\cos \theta \cos A_0 - (\lambda_u - \sin \theta) \sin A_0}{\sqrt{[(\lambda_u - (\sin(\theta))^2 + (\sin(\theta))^2)]}} \right) \quad (11)$$

The terms used in the above equation are described as angle of attack (α), initial angle of attack (A_0), azimuth location angle (θ), and local tip speed ratio (λ_u)

$$= (\lambda_u = \frac{u_u}{V_u})$$

The initial angle of attack, A_0 is assumed to be zero to represent the initial turbine blade at the azimuth position.

The following equation formulates the wind velocity relative to flow,

$$V_{ru} = \sqrt{V_u^2 \left[\left(\lambda_u - (\sin(\theta))^2 + \cos(\theta)^2 \right) \right]} \quad (12)$$

The following two equations calculate the coefficient related to tangential and normal force of turbine blade,

$$C_t = C_L \sin(\alpha) - C_D \cos(\alpha) \quad (13)$$

$$C_n = C_L \cos(\alpha) + C_D \sin(\alpha) \quad (14)$$

The drag component for the front streamside is calculated as,

$$F_u = \frac{1}{2} \sigma V_{ru}^2 [C_n \cos(\theta) - C_t \sin(\theta)] \Delta\theta \quad (15)$$

where σ is turbine solidity, and it is given as,

$$\sigma = \frac{Bc}{2\pi R} \quad (16)$$

It is dependent on the number of turbine blades, chord length, and radius of the turbine, as described in Eq. 16. From the Eq. 8 and Eq. 15 the interference factor (a_u) for the front stream part is calculated in the following ways,

$$Re = \frac{\rho V_r D}{\mu} \quad (17)$$

also,

$$\frac{1 - a_u}{a_u} = F_{ui} \quad (18)$$

where,

$$F_{ui} = \frac{Bc}{9\pi R} \int_{-\pi/2}^{+\pi/2} \frac{V_{ru}^2}{V_u^2} \sec\theta [C_n \cos(\theta) - C_t \sin(\theta)] d\theta \quad (19)$$

The inherent term of the above equation is obtained by,

$$a_u = \frac{\pi}{F_{ui} - \pi} \quad (20)$$

As each turbine blade passes through the front stream a_u and rear stream part of the stream tube, the convergence a_u procedure is continual for every azimuthal location of the turbine blade. Hence, an iterative process is followed to calculate the front stream interference factor. This process continues until convergence is obtained among the present and latest values within the given limit.

$$T_{\theta u} = \frac{1}{2} \rho V_{ru}^2 (hc) R C_t \quad (21)$$

The wind turbine rotates through 360° angles when it completes one rotation. In the present analysis number of stream tubes with an equal angle of 5° is placed in the complete one rotation of the turbine. This turbine rotation is divided into two parts front steam and rear stream. Wind flows through stream tubes and comes in contact with each blade to generate drag and lift on the turbine's blades to generate torque and power output from the wind turbine. This turbine power is calculated by using the following equation,

$$T_{avu} = \frac{\rho hc BR}{4\pi} \int_{-\pi/2}^{+\pi/2} V_{ru}^2 C_t d\theta \quad (22f)$$

The average torque coefficient (C_{qavu}) of the upstream half is given as,

$$C_{qavu} = \frac{T_{avu}}{\frac{1}{2} \rho A R V_{\infty u}^2} \quad (23)$$

The following equation calculates the power coefficient (C_{pu}) for the front stream part,

$$C_{pu} = C_{qavu} \times \lambda \quad (24)$$

In the above equation term, the tip speed ratio λ is used, given by the equation as $\lambda = \frac{u}{V_{\infty u}}$.

where u is peripheral velocity and $V_{\infty u}$ is free stream velocity.

Similarly, the power coefficient of the turbine at the rear steam tube area is obtained as,

$$C_{pd} = C_{qavd} \times \lambda \quad (25)$$

The turbine's gross or total power coefficient is obtained by adding power coefficients of the front stream and rear stream parts. It is obtained by the following equation,

$$C_p = C_{pu} + C_{pd} \quad (26)$$

An analytical, computational method is used for the performance analysis of wind turbines. A Matlab program is used for this analysis. The data table as given in the reference (Sheldahl and Klimas, 1981) [23] is used for the input required to calculate the power coefficient of the wind turbine. The geometrical parameters as described in Table 1 are used in the present computational method to calculate the performance parameters of the turbine.

The turbine's performance with different parameters is studied and analyzed by the referred momentum model. Based on analytical model results, the dimensions of a wind turbine are considered. The design terms and wind turbine specifications are given in Table 1.

Table 1: Specifications of turbine

| Design Terms |
|--|
| Straight blade height, h = 600 mm |
| Diameter of Darrieus turbine, D = 600 mm |
| Chord, c = 150 mm |
| Number of blades, B = Four |
| Profile of straight blade = NACA0018 |

3. VARIABLE PITCHING OF TURBINE BLADES

The straight blade Darrieus turbine is lift based turbine and is generally considered to control at a small angle of attack. If a large angle of attack exists, the separation of wind flow from the blade's trailing edge occurs, which experiences a stall. When the wind turbine rotates, each blade undergoes a cyclic variation of the angle of attack due to wind inflow and rotational speeds. The airfoil blade experiences stall due to a large cyclic variation of

the angle of attack at the low or intermediate tip speed ratio. The stall effect is more at the low blade velocity of the turbine due to large variation in the angle of attack. Therefore, the fixed-pitch rotor generates negligible torque due to low lift force and hence cannot start the turbine on its own. In a present research paper, the best blade pitching positions at different azimuthal positions for different λ are designed and developed to minimize the angle of attack variations to reduce the stall effect and get the maximum tangential force for the improvement of the performance of the turbine.

There is a unique blade position at a particular blade angle which gives maximum tangential force and power output. The power coefficient of the turbine will increase if the wind turbine is operated with these blade pitch angles. Figure 2 represents the best blade pitching position and its schedule defined and designed by the six best pitching curves (pitch curve 1 to pitch curve 6) for λ in $0 < \lambda < 3$. The six pitching curves are illustrated in Figure 2. These pitching curves are designed for NACA 0018 airfoil. Therefore, it applies to NACA 0018 airfoil. It is not for one Reynolds number. The Reynolds number is related to the relative velocity of wind, and it changes with the azimuthal position of turbine blades. Therefore, the pitching curves illustrated in Figure 2 are designed for different Reynolds numbers. It is considered in the calculations by the computational method (DMST model). The Reynolds number is given as,

$$Re = \frac{\rho V_r D}{\mu} \quad (27)$$

In the above equation, terms are used as ρ = mass density, μ = viscosity, V_r = wind relative velocity, and D = diameter of the turbine.

Analytical analysis for the optimization of pitching curves is carried out, and according to analytical results, the maximum power coefficient is reported by the pitch curve 5 than the other pitch curves 1 to pitch curve 4 for the tip speed ratio range from 0 to 3 ($0 < \lambda < 3$). Therefore, the pitching schedule of the turbine blade is done as per the pitch angle considered in the pitch curve 5 as shown in Figure 2.

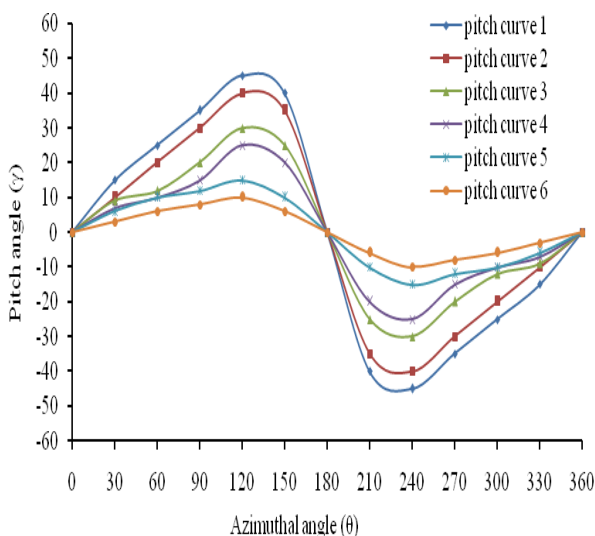


Figure 2. Pitching Schedule Curves for different λ

Therefore, for the present analysis, pitch curve 5 is selected to design and fabricate the cam and follower pitch control method for a wind turbine.

In the case of the variable pitch method, the wind turbine consists of two parallel axes; one axis on which the turbine rotates, and turbine blades are allowed to pitch on the other axis. The turbine's shaft is one axis, and the rod passing through the blade is considered the other axis, and these two are parallel to each other. This parallel axis arrangement is provided to control the predetermined pitch angles. The turbine blades' angles are changed with this parallel axis to get the maximum power from wind energy. The pitching control mechanism is developed for changing the angle of attack of wind velocity when it strikes the blades of the wind turbine.

3.1 Cam and follower pitching mechanism

The cam and follower pitching mechanism has been designed and developed, which consists of components like; Cam and follower, slider assembly, pull rod, tension spring, pull rod connector, main pitching pivot point, and pull rod pivot point. The graphical representation of various components of the turbine blade pitching method is shown in Figure 3.

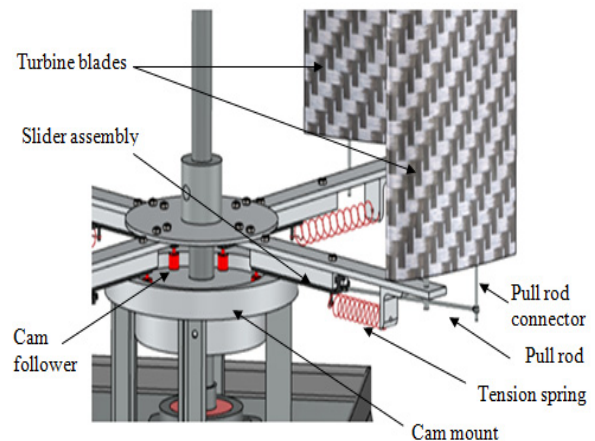


Figure 3. Graphical representation of blade pitching method

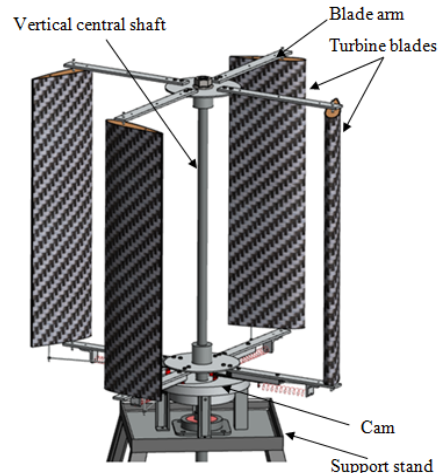


Figure 4. Wind turbine with various components

The cam is designed to get the required pitch angle of the blade at the different azimuthal positions of the turbine blade when it rotates. The cam shape is obtained

based on the requirements of blade pitching angles. The predetermined pitch angle decides the contour of the cam. Any point in the contour line of the cam chooses the pitch angle of the blade by rolling the cam follower on the contour line of the cam. Thus, the predetermined pitch angles decide the cam shape. The pitching angles of blades at various azimuthal positions are predetermined, and these angles are obtained by the displacement mechanism of the follower over the cam surface. The different wind turbine components and linkages are shown in Figure 4 and Figure 5. Figure 6 represents the displacement diagram for cam design, and Figure 7 shows the cam profile and displacement of slider assembly. The cam profile is obtained from the displacement diagram when the follower rolls on the cam surface at different azimuth angles from 0° to 360° with a regular interval of 30° .

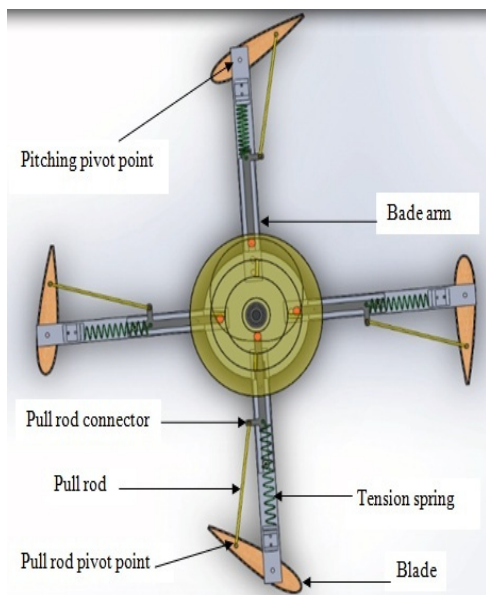


Figure 5. Different linkages for wind turbine

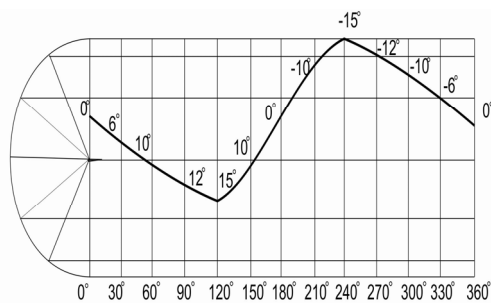


Figure 6. Cam design displacement diagram

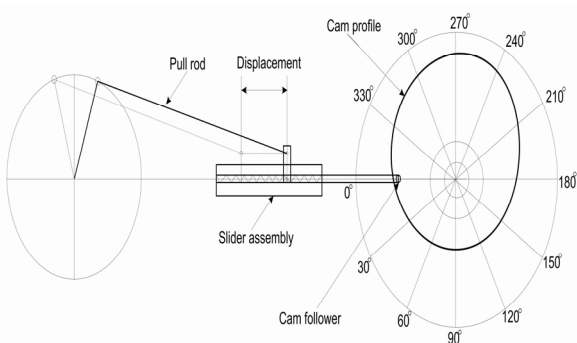


Figure 7. Cam profile and displacement of slider assembly

4. TESTING OF TURBINE MODEL

Based on the results from the analytical model, the optimized turbine is fabricated for experimentation and testing. The optimized turbine with cam and follower pitching mechanism is built and tested in open wind flow artificially created by the axial fan.

The turbine model with specifications as given in Table 1 is fabricated. The turbine consists of four blades connected to the vertical central shaft of the turbine through the support arm. The turbine assembly and cam and follower mechanism are mounted on a support stand with two roller bearings. The base structure, turbine shaft, cam, and cam mount are mild steel. The blade support arm and slider assembly are made of aluminum.

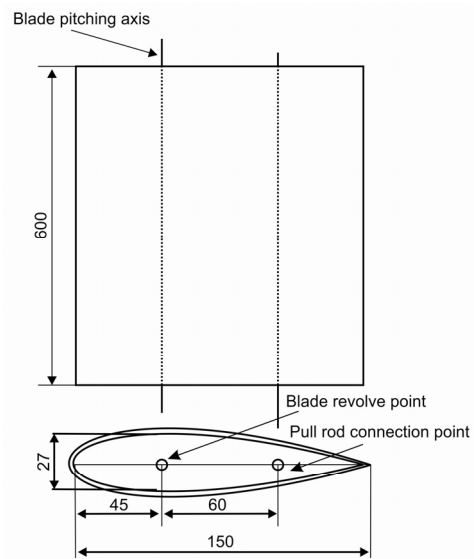


Figure 8. Turbine blade details

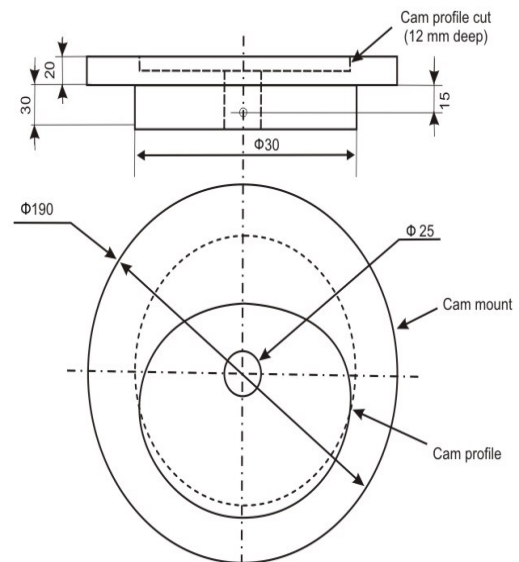


Figure 9. Cam profile and cam base

An alternator is coupled to the turbine shaft and is mounted on the base house of the support stand. The turbine model is designed based on structural considerations for centrifugal forces. The airfoil blades are designed for strength and stiffness with lightweight and smoothness. The blades are constructed from wooden

and thermocol strips with two core holes to fit two aluminum rods. These wooden and thermocol strips are alternatively lengthwise sandwiched and covered with an aluminum sheet and a carbon fiber sheet. The carbon fiber sheet is used to make the blade surface smooth. The blades are streamlined with asymmetrical NACA0018 airfoil profile shapes. Figure 8 shows the airfoil blade cross-section used for the turbine model. Figure 9 shows the shape of the cam and is fabricated with 12 mm deep cut inside the cast iron circular plate. The CNC lathe machine with a good surface finish to roll the cam follower freely on the smooth cam surface obtains the cam profile surface.

4.1 Experimental setup and testing of turbine model

Figure 10 represents the photograph of the experimental setup for testing the variable pitch turbine model with a cam and follower mechanism. The experimental setup consists of a turbine, electrical alternator, axial fan, and measuring instruments. The experiment was conducted in an open wind flow created by the five-bladed axial fan. The air velocity from one ms^{-1} to ten ms^{-1} was adjusted by changing the speed of the axial fan. The wind speed was measured by a wind anemometer placed at 0.5 m from the axial fan and at the center of wind flow. The turbine model is fitted on the support stand with a central shaft mounted on two ball bearings. The bottom part of the turbine shaft is connected to a DC alternator (Model 48 Volts, 4.2 Amp, and 200 Watt) with a rectifier. The electrical energy output generated by the turbine is obtained from the DC alternator. The electrical circuit contains an ammeter, voltmeter, and rheostat connected to the DC alternator. The rheostat is connected parallel to the voltmeter used to give resistance, which is applied as a load on the rotor shaft for measurement of power at the output shaft of the turbine for different speeds. The details of the test flow and electric circuit are shown in Figure 11. The current and voltage are recorded with an ammeter and voltmeter, respectively, to calculate the electrical power output at various loads and speeds of the turbine. The DC alternator efficiency is 80 %.

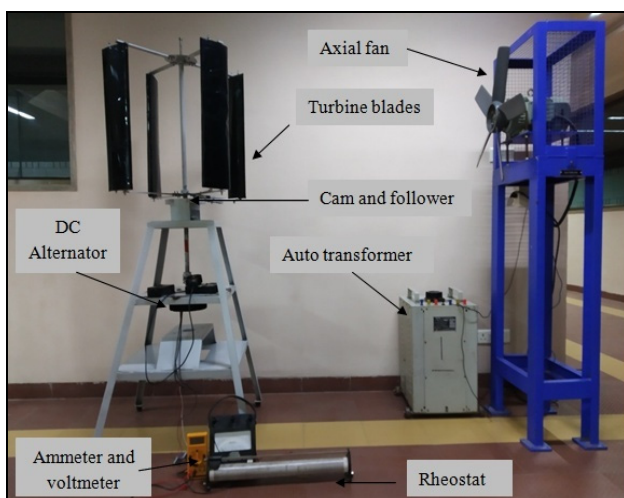


Figure 10. Photo of the experimental setup

The present turbine model is optimized analytically by using these simulation codes; then, this optimized

turbine model is fabricated and tested for its performance. The analytical model simulation code validation is carried out with the results of the turbine used by Paraschivoiu et al., 2009[12]. These results are closer, with variations up to 2 % to 5 %, as shown in Figure 12.

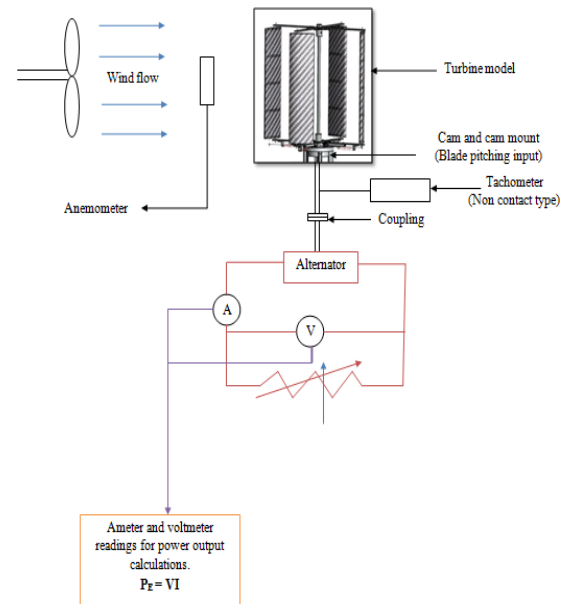


Figure 11. Test apparatus and flow diagram

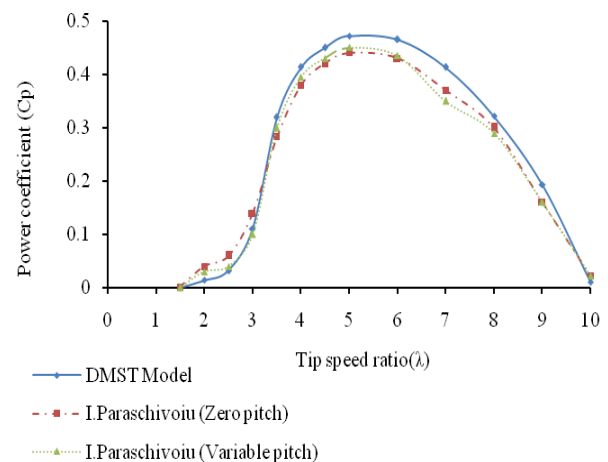


Figure 12. Turbine result validation

5. RESULTS AND DISCUSSIONS

The variable pitch turbine with cam and follower pitching mechanism is tested for different air velocities by changing velocity from one ms^{-1} to ten ms^{-1} for the constant load. This type of wind turbine initially starts on its own at low air velocity, and it takes speed and its rotations per unit time increase with the increase of air velocity. The maximum turbine speed of 810 rpm is attained at an air velocity of ten ms^{-1} . Test results show that the maximum experimental C_p of 0.36 is obtained at a wind speed of 9 m/s as shown in Figure 13.

The turbine's performance is also measured from the test conducted by varying the load at a constant air velocity of 4, 6, 8, and 10 ms^{-1} . The results of the test are recorded. The pattern of test results for different rotor speeds at various air velocities is shown in the figures from Figure 14 to Figure 17. The test results

show that the experimental C_p increases with λ , and the maximum experimental C_p of about 0.35 is obtained at $\lambda = 2.5$ for a given wind speed range. The experimental results also show that the large variety of 30 % to 35 % in the measured C_p and analytical C_p of this type of variable pitch wind turbine is recorded and represented in the plot as indicated in Figures 13, 14, 15, 16, and 17. This large variation was observed in the measured C_p and the analytical C_p for variable pitch turbine due to friction created by a various cam and follower pitching mechanism components.

The DMST model as the computational method is used for the present analysis. In this model, simplified assumptions are made. The validation of the computational approach used in the study is done with the turbine results used by Paraschivoiu et al., 2009[11]. The assumptions used for the present analysis are given below.

- Airflow is steady and does not vary with time.
- Flow is inviscid. The viscosity of a fluid is constant in the stream tube flow.
- Flow is incompressible and irrotational. The mass density of air is constant over the flow of the turbine. Flow is irrotational as molecules of airflow along the streamline of fluid.
- The vorticity of fluid and stall effect is neglected as flow is attached to the wind turbine blades.

Therefore, large differences between computed and measured values (up to 35%) are reported in the paper. This difference is due to the friction offered by Cam and Follower Pitching Mechanism.

Friction losses are not much high. The pitching mechanism friction is only between the roller and cam profile in the cam and follower and in the slider assembly. This source of friction can be reduced by using a polished cam profile surface and proper alignment of the slider assembly. Further friction can be reduced by providing lubricating oil at meeting assembly surfaces. The main purpose of the pitching mechanism is to make the turbine rotate when wind flows on airfoil blades. It is happened due to increased lift force on airfoil blades.

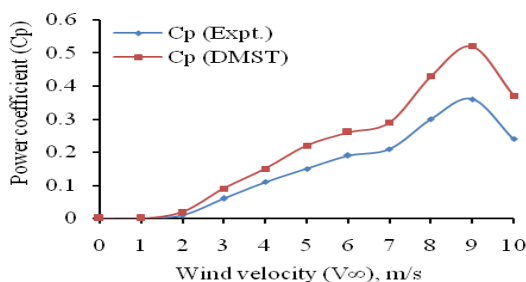


Figure 13. C_p versus V_∞ for variable pitch turbine

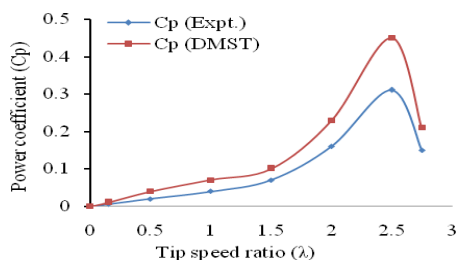


Figure 14. C_p versus λ at $V_\infty = 4$ m/s

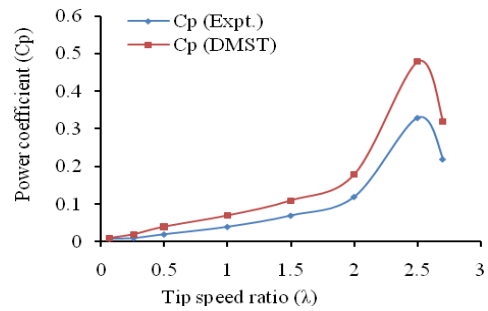


Figure 15. C_p versus λ at $V_\infty = 6$ m/s

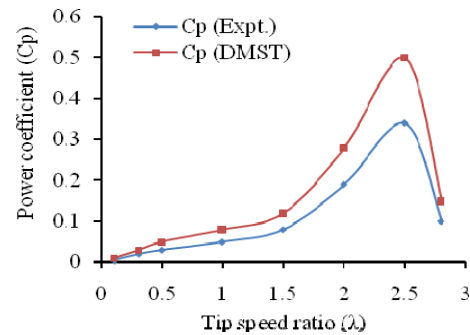


Figure 16. C_p versus λ at $V_\infty = 8$ m/s

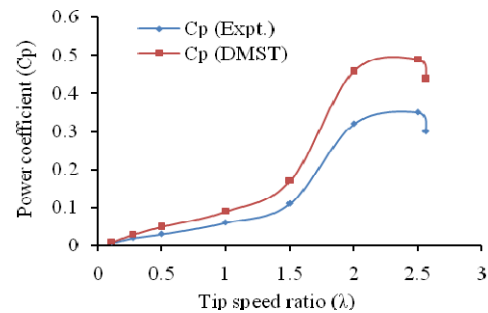


Figure 17. C_p versus λ at $V_\infty = 10$ m/s

6. CONCLUSIONS

- The turbine with a cam and follower pitching mechanism is tested for different wind speeds. The test results show that the experimental C_p increases with λ , and the maximum experimental C_p of about 0.35 is obtained at $\lambda = 2.5$ at 10 ms^{-1} wind speed. The experimental $C_p = 0.35$ which is less than the analytical $C_p = 0.49$ for $\lambda = 2.5$ at wind speed of 10 m/s. It is concluded from the test results that the experimental C_p is about 30 % to 40 % less than the analytical C_p . This large variation of power coefficient in experimental C_p and analytical C_p is observed because of the frictional losses due to various components of the cam and follower pitching mechanism.
- Experimental results show that this type of pitching control method enhances the power output and C_p of a wind turbine. The present analytical and experimental performance of the turbine indicates that this type of variable pitching of turbine blades will improve C_p for different λ in the value of tip speed ratio as $0 < \lambda < 3$.
- The main source of friction is ball bearings and cam follower pitching mechanism. The cam and follower consist of a slider mechanism, linkages, and tension

springs. The various components in the turbine assembly slide on each other and create friction. Some power is lost to overcome the friction. The linkages and springs used in the cam and follower pitching mechanism consume some of the turbine torque. Collectively, this resistive torque results in a lower power coefficient of the turbine with cam and follower pitching mechanism at various tip speed ratios and wind speed. This resistive torque is significant when the turbine speed increases as friction increase with the speed of the turbine.

- 4) The analytical and experimental results of the research work will be helpful for the design and fabrication of variable pitch turbines. The results are also beneficial in the turbine manufacturing area. The turbine model is easy to fabricate, costs less, and is pollution-free. It is suggested as ideal for household applications for power generation in developing countries where sufficient wind is available in rural and urban areas.

ACKNOWLEDGMENT

The authors thank BCUD Savitribai Phule Pune University for a research grant to develop an experimental setup. The authors are thankful to the Management and Principal of Dr. D.Y. Patil Institute of Technology, Pimpri, Pune, for their full support and cooperation in this project.

REFERENCES

- [1] Biadgo, A. M., Aynekulu, G.: Aerodynamic Design of Horizontal Axis Wind Turbine Blades, *FME Transactions*, Vol. 45 No 4, pp 647-660, 2017.
- [2] Rasuo, B., Bengin, A.: Optimization of Wind Farm Layout, *FME Transactions*, Vol. 38 No 3, pp 107-114, 2010.
- [3] Rasuo, B., Bengin, A., Veg, A.: On Aerodynamic Optimization of Wind Farm Layout, *PAMM*, Vol. 10, Issue1, pp. 539–540, 2010.
- [4] Samanoudy, M., Ghorab, A. A., and Youssef, Z.: Effect of some design parameters on the performance of a Giromill vertical axis wind turbine, *Ain Shams Engineering Journal*, 1, 85-95, 2010.
- [5] Kalakanda, A. S., and Nallapaneni, M. K.: Vertical axis wind turbine- aerodynamic modeling and its testing in wind tunnel. *Procedia Computer Science*, 1017-1023, 2016.
- [6] Ivanov, D. T., Simonović, M. A., and Svorcan, S. J., and Peković, M. O.: VAWT Optimization Using Genetic Algorithm and CST Airfoil Parameterization, *FME Transactions*, Vol. 45, No. 1, pp 26-31, 2017.
- [7] Biadgo, A. M., Aleksandar, S., Dragan, K., and Slobodan, S.: Numerical and Analytical Investigation of Vertical Axis Wind Turbine, *FME Transactions*, pp. 49-58,2013.
- [8] Tareq, A. I., Sattar, A., Omar, A. A., and Yasir, A. A.: Energy Recovery of Moving Vehicles' Wakes in Highways by Vertical Axis Wind Turbines, *FME Transactions*, pp. 557-565, 2020.
- [9] Svorcan, J., Trivković, Z., Ivanov, T., Baltić, M., and Peković, O.: Multi-objective Constrained Optimizations of VAWT Composite Blades Based on FEM and PSO, *FME Transactions*, Vol. 47, No. 4, pp. 887-893, 2019.
- [10] Rasuo, B., Dinulovic, M., Veg, A., Grbovic, A., and Bengin, A.: Harmonization of new wind turbine rotor blades development process: A review, *Renewable and Sustainable Energy Reviews*, Vol. 39, November 2014, pp. 874-882, doi: 10.1016/j.rser.2014.07.137.
- [11] Bianchini, A., Balduzzi, F., John, M. R., Joaquim, P., Michael, J., Giovanni, F., and Ferrari, L.: An Experimental and Numerical Assessment of Airfoil Polars for Use in Darrieus Wind Turbines Part I: Flow Curvature Effects, *Journal of Engineering for Gas Turbines and Power*, Vol. 138, pp. 032601-2, 2016
- [12] Paraschivoiu, I., Trifu, O., and Saeed F.: H-Darrieus wind turbine with blade pitch control, *International Journal of Rotating Machinery*, Volume ID 5053343, 2009.
- [13] Cooper, P., and Kennedy, O. C.: Development and analysis of novel vertical axis wind turbine. *Australian and New Zealand Solar Energy Society*, 1-9, 2004.
- [14] Kirke, B. K., and Benoit, P.: Predicted and measured performance of a vertical axis wind turbine with passive variable pitch compared to fixed pitch. *Journal of Wind Engineering*, 1-27, 2016.
- [15] Elkhoury, M., Kiwata, T., and Aoun, E.: Experimental and numerical investigation of three-dimensional vertical axis and wind turbine with variable pitch. *Journal of Wind Engineering and Industrial Aerodynamics*, 139, 111-123, 2015.
- [16] Zhang, L., Liang, Y., LIU, X., and Jian, G.: Effect of blade pitch angle on aerodynamic performance of straight-bladed vertical axis wind turbine. *Springer*, 21:1417-1427, 2014.
- [17] Jain, P., and Abhishek, A.: Performance prediction and fundamental understanding of small scale vertical axis wind turbine with variable amplitude blade pitching. *Journal of Renewable Energy*, 97-113, 2016.
- [18] Liang, Y., Zhang, L., and Zhang F.: Blade pitch control of straight-bladed vertical axis wind turbine, *Springer*, 23:1106-1114, 2016.
- [19] Carlos, M. X., Jose, C. P., and Michele, T.: Geothermal parameter influencing the aerodynamic efficiency of small scale self-pitch high-solidity VAWT. *ASME*, Vol. 138/031006-1, 2016.
- [20] Edwards, J. M., Lousis A. D., and Howell, R. J.: Novel experimental power curve determination and computational method for the performance analysis of vertical axis wind turbines, *ASME*, Vol. 134/031008-1, 2012.
- [21] Islam, M., Ting, D. S.K., and Fartaj, A.: Aerodynamic models for Darrieus-type straight-bladed vertical axis wind turbines. *Renewable and Sustainable Energy Reviews*, 12, 1087-1109. 2008.
- [22] Beri, H., and Yao, Y.: Double multiple stream tube model and numerical analysis of vertical axis wind turbine. *Scientific Research, Energy and Power Engineering*, 3, 262-270, 2011.
- [23] Sheldahl, R. E., and Klimas, P.C.: Aerodynamics characteristics of Seven Symmetrical Airfoil Sections through 180-degree angle of attack for use

NOMENCLATURE

| | |
|-----------|--|
| ρ | Density of air (kg/m ³) |
| μ | Dynamic viscosity (kg/m.s) |
| c | Blade chord length (m) |
| R | Radius of turbine (m) |
| D | Diameter of turbine (m) |
| H | Height of turbine (m) |
| h | Height of blade (m) |
| σ | Turbine solidity |
| B | Number of blades |
| C_p | Power coefficient |
| C_D | Coefficient of drag |
| C_L | Coefficient of lift |
| θ | Azimuth angle (Degree) |
| α | Angle of attack (Degree) |
| u | Blade velocity (m/s) |
| λ | Tip speed ratio |
| C_n | Normal force coefficient |
| C_t | Tangential force coefficient |
| HAWT | Horizontal Axis Wind Turbine |
| VAWT | Vertical Axis Wind Turbine |
| DMST | Double Multiple Stream Tube |
| TSR | Tip Speed Ratio |
| NACA | National Advisory Committee for Aerodynamics |

АНАЛИЗА ПЕРФОРМАНСИ ВЕТРОТУРБИНЕ МАЛЕ ВЕЛИЧИНЕ СА ПРОМЕНЉИВИМ НАГИБОМ ВЕРТИКАЛНЕ ОСЕ

Р.К. Каваде, П.М. Гаонгакар

У овом раду, метода променљивог нагиба се користи за побољшање излазне снаге ветротурбине са вертикалном осовином (ВАВТ) за производњу електричне енергије како би се делимично задовољиле енергетске потребе за употребу у домаћинству на месту где је доступан континуирани проток ветра. Турбине са унапред подешеним или непроменљивим нагибом не могу да се покрену саме због негативне тангенцијалне силе која делује на лопатице турбине.

Због тога се уводи метода променљивог нагиба да би се решио стартни проблем ветротурбина и повећала ефикасност турбине у виду коефицијента снаге. За ову анализу је коришћена метода променљивог корака брега и пратиоца. У овом истраживачком раду, аналитичка анализа је урађена помоћу цевног модела импулсног тока названог ДМСТ модел. Модел турбине је тестиран, а резултати испитивања показују да коефицијент снаге (C_p) расте са односом брзине врха, а максимални коефицијент снаге од око 0,35 добија се при $\lambda = 2,5$ при брзини ветра од 10 м/с.